International Journal of GEOMATE, Jan., 2024 Vol.26, Issue 113, pp.98-106
ISSN: 2186-2982 (P), 2186-2990 (O), Japan, DOI: https://doi.org/10.21660/2024.113.g13317
Geotechnique, Construction Materials and Environment

ESTIMATING NATURAL VIBRATION CHARACTERISTICS OF BRIDGE CABLES BASED ON N4SID SUBSPACE METHOD

* Aiko Furukawa[1] and Minjiu Jiang [1]

[1] Department of Urban Management, Kyoto University, Japan

*Corresponding Author, Received: 23 June 2023, Revised: 22 Nov. 2023, Accepted: 01 Dec. 2023

ABSTRACT: Cable maintenance is important for cable structures such as cable-stayed and Nielsen-Lohse bridges. In the current maintenance practice, cable tension is estimated from the lower mode natural frequencies of the cable. It is theoretically possible to estimate the bending stiffness of the cable and the parameters of the dampers installed on the cable if the higher mode natural frequencies, damping factors, and mode shapes are available. Conventionally, the natural vibration characteristics of the cables are estimated manually from the acceleration Fourier spectrum. The estimation accuracy of the lower mode natural frequencies is high. However, the estimation accuracy of the higher mode natural frequencies is not high, and the estimation accuracy of damping factors and mode shapes is low irrespective of modal order. In this paper, the N4SID, one of the subspace methods, is adopted to estimate the natural vibration characteristics of the cables. The N4SID is applied to numerical and experimental results of bridge cables to investigate the estimation accuracy. The numerical investigation found that the accuracy of the natural frequencies and damping factors is high, the accuracy of mode shape is high in the cable without a damper, and the accuracy of mode shape is only high for the limited low modes and low for the other mode in the cable with a damper. The experimental investigation found that the N4SID has better accuracy than the conventional estimation method.

Keywords: Cable, Natural vibration characteristics, Estimation, Subspace method, N4SID, Fourier spectra

1. INTRODUCTION

Structural health monitoring [1][2] is a technique that captures structural health conditions based on their vibration characteristics. Accelerometers are generally used, and natural vibration characteristics such as natural frequencies, damping factors, and mode shapes are estimated from the measured accelerations, which are then used to evaluate the structural health condition.

The natural frequency is the easiest to measure among the natural vibration characteristics. The natural frequency is generally estimated by reading the dominant frequency of the acceleration Fourier spectrum. In the maintenance of cable bridges, such as cable-stayed bridges [3][4][5][6] and Nielsen-Lohse bridges [7][8][9], cable tension is estimated from the natural frequencies of the cable. The cable tension is sensitive to the lower mode natural frequencies, while the bending stiffness of the cable is sensitive to the higher mode natural frequencies. Since estimating the higher mode natural frequencies from acceleration responses is difficult, only tension is estimated and used for cable maintenance. If the higher mode natural frequencies can be estimated accurately, the bending stiffness can be estimated, and the detection of cable damage becomes possible.

As for the damping factor, the half-power method [10] and the random decrement method [11] are well-known estimation methods. In both methods, only one mode of interest is extracted, and the theory based on a single-degree-of-freedom system is applied even though the structure is the multi-degree-of-freedom system. Therefore, the estimated damping factors have large variations [12]. Recently, dampers have been installed on cables of cable-stayed bridges to suppress aerodynamic vibration, and it has become important to maintain dampers. However, since damper parameters are insensitive to natural frequencies, estimation of damper parameters from natural frequencies is difficult [3][4][6]. If the damping factors of cables can be estimated accurately, the maintenance of dampers becomes possible.

Mode shapes correspond to the Fourier amplitudes at natural frequencies and are usually estimated manually from the Fourier spectra. Estimated mode shape includes errors due to calculation measurement errors [13]. In cable maintenance, it was found that the mode shapes can be expected to improve the estimation accuracy of the cable tension and bending stiffness, and damper parameters [5].

Based on the above, if the estimation accuracy of natural frequencies, damping constants, and mode shapes can be improved, it will contribute to the maintenance of cable structures.

In many studies on structural health monitoring, natural vibration characteristics are manually estimated from acceleration Fourier spectra. In contrast to such methods, system identification

based on subspace methods [14] is a method for obtaining the system matrices of a state space model directly from input-output data. Natural vibration characteristics can be indirectly estimated from the estimated system matrices. Yoshimoto et al. [15] and Nagano et al. [16] applied the subspace method to the building to identify the stiffness and dynamic parameters during earthquakes. Hida et al. [17] compared the identification accuracy of various subspace methods on natural frequencies and damping factors of super high-rise RC structures during the 2011 off the Pacific Coast of Tohoku Earthquake. Ishii et al. [18] used the subspace method to estimate the damping characteristics of an entire bridge system.

As described above, the subspace method has recently been applied to buildings and bridges during earthquakes, but no past research exists that applied the subspace method to the bridge cable. The purpose of this study is to investigate whether the N4SID (Numerical algorithms for Subspace State Space System Identification) [19], which is currently the most popular subspace method, can estimate the natural vibration characteristics of cables accurately and whether the subspace method is superior to the conventional manual estimation method based on the Fourier spectrum.

2. RESEARCH SIGNIFICANCE

The significance of the study is that the N4SID is firstly applied to bridge cables, and the estimation accuracy of the natural vibration characteristics of cables is investigated through numerical simulation and a field experiment. The numerical investigation compared the estimation accuracy between cables with and without measurement error and with and without a damper. The effect of a damper on the estimation accuracy was investigated. In the experimental investigation, the estimation accuracy of the N4SID and the conventional method was compared, and the superiority of the N4SID was discussed.

3. METHOD

3.1 Natural Vibration Characteristics Estimation from State Space Model

The state-space representation of an m-input l-output discrete-time linear time-invariant system is described as follows.

$$\begin{cases} x(k+1) = A_d x(k) + B_d u(k) + w(k) & (1) \\ y(k) = C_d x(k) + D_d u(k) + v(k) & (2) \end{cases}$$

$x(k)$, $u(k)$, and $y(k)$ are the state vector, input vector, and output vector at step k. $w(k)$ and $v(k)$ are the process noise vector and measurement noise vector. A_d, B_d, C_d, and D_d are the system matrices. Eq. (1) is the state equation, and Eq. (2) is the observation equation. System identification estimates the system matrices from the input vector $u(k)$ and output vector $y(k)$.

The system matrices are expressed as follows by converting an equation of motion into a state-space representation.

$$A_d = \exp\left(\begin{bmatrix} 0 & I \\ -M^{-1}K & -M^{-1}C \end{bmatrix} \Delta t\right) \quad (3)$$

$$B_d = \begin{bmatrix} 0 \\ M^{-1} \end{bmatrix} \quad (4)$$

$$D_d = 0 \quad (5)$$

M, C, and K are the mass, damping, and stiffness matrices. The natural frequency f_j, damping factor h_j, and mode shape ϕ_j of the j-th mode are expressed as follows using the j-th eigenvalue λ_d^j and eigenvector V_d^j of matrix A_d, sampling period Δt, and matrix C_d.

$$A_d V_d^j = \lambda_d^j V_d^j \quad (6)$$

$$f_j = Im\{\log(\lambda_d^j)\}/2\pi\Delta t \quad (7)$$

$$h_j = \frac{-Re(\log(\lambda_d^j))}{\sqrt{\{Re(\log(\lambda_d^j))\}^2 + \{Im(\log(\lambda_d^j))\}^2}} \quad (8)$$

$$\phi_j = C_d V_d^j \quad (9)$$

The natural vibration characteristics of the cable are estimated from the system matrices, A_d and C_d. The subspace method identifies the system matrices.

3.2 Extended observability matrix

Let us define $Y_r(k)$ and $U_r(k)$ as follows.

$$Y_r(k) = \begin{bmatrix} y(k) \\ y(k+1) \\ \vdots \\ y(k+r-1) \end{bmatrix} \in \mathcal{R}^{pr\times 1} \quad (10)$$

$$U_r(k) = \begin{bmatrix} u(k) \\ u(k+1) \\ \vdots \\ u(k+r-1) \end{bmatrix} \in \mathcal{R}^{mr\times 1} \quad (11)$$

Then, $Y_r(k)$ can be written as follows.

$$Y_r(k) = O_r x(k) + S_r U_r(k) + V(k) \quad (12)$$

where O_r, S_r, and $V(k)$ are

$$O_r = \begin{bmatrix} C_d \\ C_d A_d \\ \vdots \\ C_d {A_d}^{n-1} \end{bmatrix} \quad (13)$$

$$S_r = \begin{bmatrix} D_d & 0 & \cdots & 0 & 0 \\ C_d B_d & D_d & \cdots & 0 & 0 \\ \vdots & \vdots & \ddots & \vdots & \vdots \\ C_d {A_d}^{r-2} B_d & C_d {A_d}^{r-3} & \vdots & C_d B_d & D_d \end{bmatrix} \quad (14)$$

$$V(k) = C_d {A_d}^{r-2} B_d\, w(k) + CA^{r-3} B\, w(k+1) + \cdots + Cw(k+r-2) + v(k+r-1) \quad (15)$$

Assuming that $u(k)$ and $y(k)$are available for $k = 1, 2, \cdots, N+r-1$, we obtain the following equation.

$$Y = [Y_r(1) \quad Y_r(2) \quad \ldots \quad Y_r(N)] \in \mathcal{R}^{pr\times N} \quad (16)$$

$$X = [x(k) \quad x(2) \quad \ldots \quad x(N)] \in \mathcal{R}^{n\times(N-k+1)} \quad (17)$$

$$U = [U_r(1) \quad U_r(2) \quad \ldots \quad U_r(N)] \in \mathcal{R}^{mr\times N} \quad (18)$$

$$V = [V(1) \quad V(2) \quad \ldots \quad V(N)] \in \mathcal{R}^{p\times N} \quad (19)$$

From Eqs. (12) and (16)-(20), the following equation is obtained.

$$Y = O_r X + S_r U + V \quad (20)$$

Next, we consider estimating the extended observability matrix O_r and removing the U term and the noise term V from Eq. (20).

Let be $\Pi_{U^T}^{\perp} \in \mathcal{R}^{N\times N}$ as follows.

$$\Pi_{U^T}^{\perp} = I - U^T(UU^T)^{-1}U \quad (21)$$

Multiplying U to Eq. (21) from the left side, we obtain

$$U\Pi_{U^T}^{\perp} = U - UU^T(UU^T)^{-1}U = 0 \quad (22)$$

Therefore, the matrix $\Pi_{U^T}^{\perp}$ is the orthogonal projection of the matrix U. We multiply $\Pi_{U^T}^{\perp}$ to Eq. (20) from the right side to eliminate U.

$$Y\Pi_{U^T}^{\perp} = O_r X\Pi_{U^T}^{\perp} + V\Pi_{U^T}^{\perp} \quad (23)$$

To eliminate the last term in Eq. (23), we use the matrix $\Phi \in \mathcal{R}^{s\times N}$, where Φ is defined using the input $u(k)$ and the output $y(k)$ as follows.

$$\phi_s(k) = \begin{bmatrix} y(k-1) \\ \vdots \\ y(k-s_1) \\ u(k-1) \\ \vdots \\ u(k-s_2) \end{bmatrix} \quad (s = ps_1 + ms_2) \quad (24)$$

$$\Phi = [\phi_s(1) \quad \phi_s(2) \quad \ldots \quad \phi_s(N)] \quad (25)$$

The following equation is obtained by multiplying Φ^T to Eq. (23) from the right side and dividing by N.

$$\frac{1}{N} Y\Pi_{U^T}^{\perp}\Phi^T = \frac{1}{N} O_r X\Pi_{U^T}^{\perp}\Phi^T + \frac{1}{N} V\Pi_{U^T}^{\perp}\Phi^T \quad (26)$$

Using Eq. (21), the second term of the right-hand side of Eq. (26) can be transformed as follows.

$$\frac{1}{N} V\Pi_{U^T}^{\perp}\Phi^T = \frac{1}{N} V\{I - U^T(UU^T)^{-1}U\}\Phi^T = \frac{1}{N} V\Phi^T - \frac{1}{N} VU^T(UU^T)^{-1}U\Phi^T \quad (27)$$

Under the ergodic assumption, the sample sum converges to the expected value. Therefore, Eq. (27) can be rewritten as follows.

$$\lim_{N\to\infty} \frac{1}{N} V\Pi_{U^T}^{\perp}\Phi^T = E[V(k)\varphi_s^T(k)] - E[V(k)U_r^T(k)]E[U_r(k)U_r^T(k)]^{-1}E[U_r(k)\varphi_s^T(k)] \quad (28)$$

Assuming that U and V are independent, $E[V(k)U_r^T(k)]$=0 holds. Therefore, the second term on the right-hand side of Eq. (28) is zero. Moreover, if $V(k)$ and $\varphi_s^T(k)$ are uncorrelated, the first term on the right-hand side is zero. Therefore, the following equation is obtained.

$$\lim_{N\to\infty} \frac{1}{N} V\Pi_{U^T}^{\perp}\Phi^T = 0 \quad (29)$$

Substituting Eq.(29) to Eq.(26),

$$Y\Pi_{U^T}^{\perp}\Phi^T = O_r X\Pi_{U^T}^{\perp}\Phi^T \quad (30)$$

From the above, the extended observability matrix G is obtained as follows.

$$G = Y\Pi_{U^T}^{\perp}\Phi^T \quad (31)$$

The extended observability matrix G can be calculated from the input vector $u(k)$ and output vector $y(k)$ using Eqs. (16), (18), (22), (24), (25), and (31). System matrices can be calculated from the extended observability matrix G.

3.3 Algorithm of N4SID

Next, the following matrix is defined using weight matrices $W_1 \in \mathcal{R}^{pr\times pr}$ and $W_2 \in \mathcal{R}^{s\times\alpha}$.

$$\hat{G} = W_1 G W_2 \quad (32)$$

In the N4SID, $W_1 = I$ and $W_2 = (\Phi\Pi_{U^T}^{\perp}\Phi^T)^{-1}\Phi$ are used.

$$\hat{G} = Y\Pi_{U^T}^{\perp}\Phi^T(\Phi\Pi_{U^T}^{\perp}\Phi^T)^{-1}\Phi \quad (33)$$

Singular value decomposition of $\hat{G}$ after truncating small singular values becomes

$$\hat{G} = [U_s \quad U_w]\begin{bmatrix}\Sigma_s & 0 \\ 0 & \Sigma_w\end{bmatrix}\begin{bmatrix}V_s^T \\ V_w^T\end{bmatrix} \approx U_s\Sigma_s V_s^T \quad (34)$$

where the subscripts s and w stand for the signal and noise subspaces. Σ_s is a diagonal matrix of singular values $\sigma_1, \sigma_2, \ldots, \sigma_n$ in increasing order. The singular values constructing Σ_w are assumed to be sufficiently small and ignored.

From Eqs. (30), (31), (32), and (34), we obtain

$$O_r X\Pi_{U^T}^{\perp}\Phi^T = W_1^{-1}U_s\Sigma_s V_s^T W_2^{-1} \quad (35)$$

From Eq. (35), O_r is estimated as $\hat{O}_r = W_1^{-1}U_s$. System matrices A_d and C_d are estimated as $\widehat{A_d}$ and $\widehat{C_d}$ from Eq. (13) as

$$\widehat{C_d} = \hat{O}_r(1{:}p, 1{:}n) \quad (36)$$

$$\hat{O}_r(p+1{:}pr, 1{:}n) = \hat{O}_r(1{:}p(r-1), 1{:}n)\widehat{A_d} \quad (37)$$

3.4 Natural Vibration Characteristics Estimation using N4SID

The target structures of this study are bridge cables. The acceleration responses at multiple points on the cable after striking the cable with a hammer are used for system identification. Since the system coefficient matrix D_d is zero from Eq.

(5), only matrices A_d, B_d, and C_d are estimated. The natural vibration characteristics are estimated using acceleration responses after applying an external force. Therefore, the input vector $u(k)$ is set to 0, and acceleration responses are used as $y(k)$.

The estimation flow using the N4SID employed in this study is as follows.

[Step 1] The input vector $u(k)$ is considered to be 0, and the acceleration responses at multiple points are stored in the output vector $y(k)$.

[Step 2] Select the model order by truncating the small singular values.

[Step 3] Estimate the system matrices A_d, B_d, and C_d.

[Step 4] Estimate natural vibration characteristics from the system matrices A_d, and C_d.

4. NUMERICAL VERIFICATION

4.1 Overview

This chapter verifies the N4SID for natural vibration characteristics estimation of a bridge cable. The target structure is a cable of a cable-stayed bridge. First, natural vibration characteristics (natural frequencies, damping factors, and mode shapes) are computed by an eigenvalue analysis of the FEM and regarded as true values. Next, the acceleration responses of a cable hit by a hammer are computed by the dynamic analysis of the FEM and input into N4SID to estimate the natural vibration characteristics. The natural vibration characteristics estimated by the N4SID are compared with the true values to evaluate the estimation accuracy of the N4SID.

4.2 Analysis Model

An analysis model is shown in Fig. 1. The cable is made of steel with a density per length of 30.1 kg/m, a tension of 3300 kN, and a bending stiffness of 106 kN/m^2. The cable is 50 m long and divided into 100 elements with 101 nodes. The cable is fixed at both ends. The cable was modeled with a tensioned Euler-Bernulli beam.

The hammering position is node No. 11. The measurement points are node Nos. 11, 16, 21, and 26. A square wave with an amplitude of 1 kN and a duration of 1.0×10^{-4} s is applied at node No. 11, and acceleration responses at node Nos. 11, 16, 21, and 26 are computed and input to the N4SID.

In addition to the cable model shown in Fig. 1(a), a cable model with a damper shown in Fig. 1(b) is also considered. The damper is attached to node No. 9.

Even for the cable model without a damper, Rayleigh damping was introduced, assuming the 1st and 10th modes have a damping factor of 0.5%. The value of 0.5% was determined based on the measurement data of an actual cable. As for a cable with a damper, the damper was modeled with a spring and dashpot and set in parallel in the vertical direction. The stiffness is 237 kN/m, and the damping coefficient is 3.41 kN·s/m, so the damping factor of the lower mode becomes close to 3%.

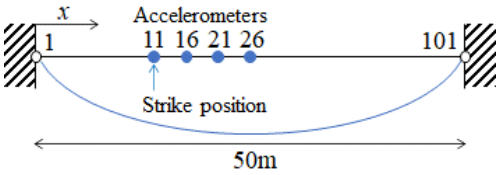

(a) Cable with no damper

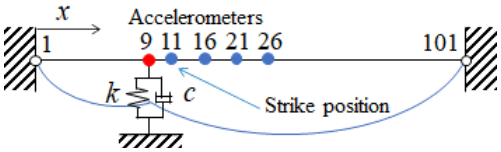

(b)Cable with damper

Fig. 1 Analysis model

Table 1 Analytical cases

	Damper	Noise	Time duration
Case A1	No damper	0 %	1-20 s
Case A2	No damper	5 %	1-20 s
Case A3	With damper	5 %	1-20 s

4.3 Analysis Case and Input Force

An analysis case is shown in Table 1. In A1 and A2, the cable model without a damper is used. No measurement error is considered in A1, and a measurement error of 5% is considered in A2. In A3, the cable with a damper model is considered, and measurement error of 5% is considered. The measurement error was modeled with Gaussian distribution with a standard deviation of 5% of the standard deviation of the acceleration response without measurement error.

The time interval of the dynamic analysis is 1.0×10^{-4} s. The square wave with amplitude 1kN was input to the cable from 1.0×10^{-4} to 2.0×10^{-4} s. Acceleration histories for 20 s are computed using the FEM. The acceleration histories from 1 to 20 s are extracted to remove the acceleration responses while hitting a cable with a hammer.

4.4 Results

4.4.1 Acceleration histories and Fourier spectra

The normalized acceleration histories for three cases are shown in Fig. 2(a). The amplitude was normalized by the largest value among the four

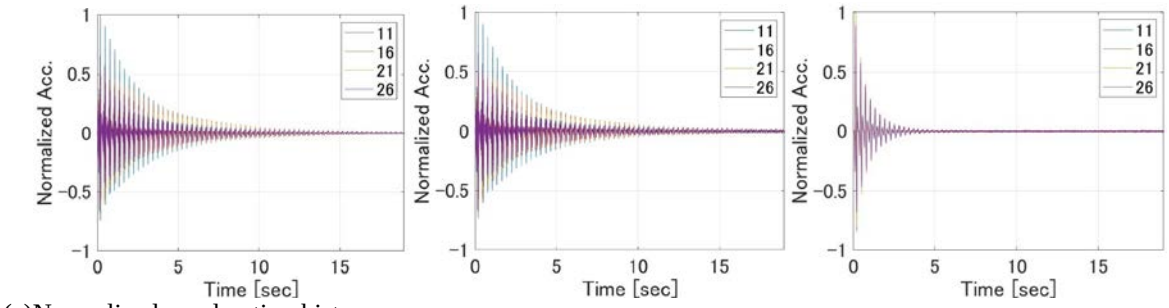

(a)Normalized acceleration history

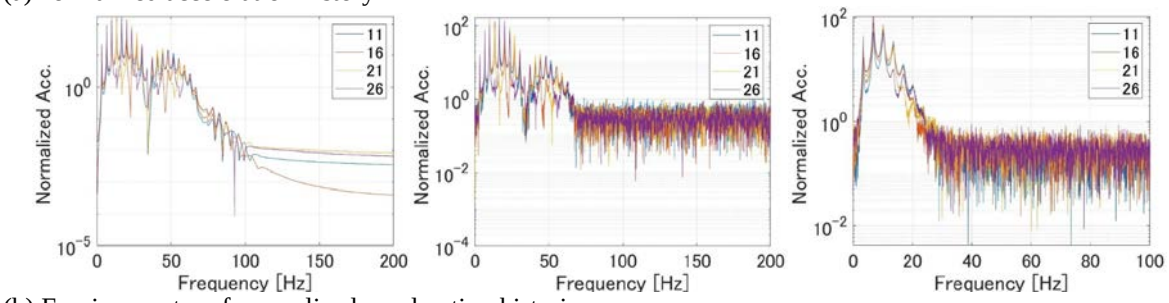

(b) Fourier spectra of normalized acceleration histories

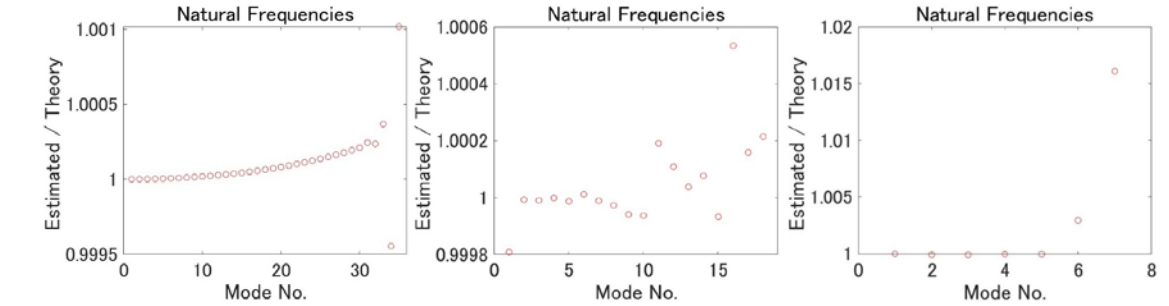

(c)Ratio of estimated natural frequency to true value

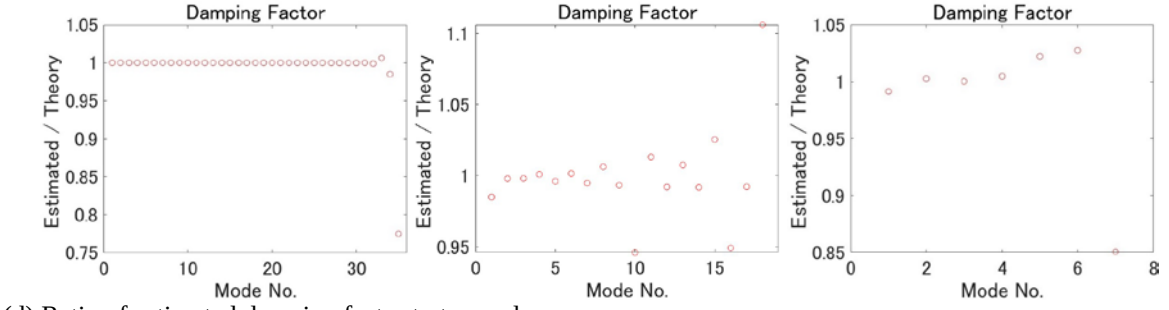

(d) Ratio of estimated damping factor to true value

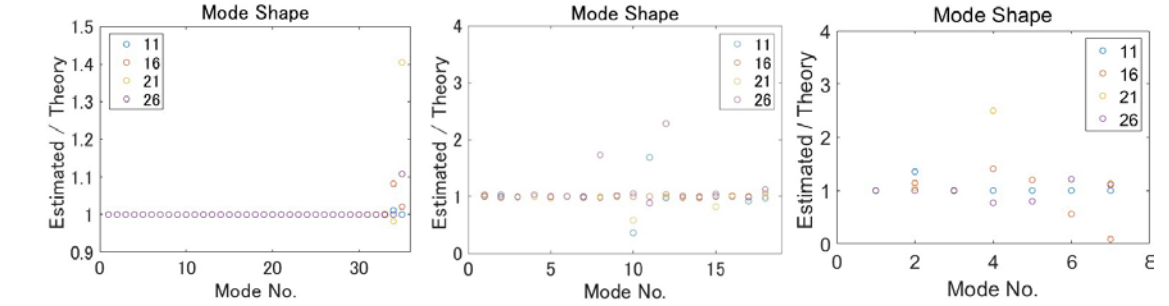

(e) Ratio of estimated mode shape to true value

Fig.2 Results of numerical verification (left: case A1, middle: case A2, right: case A3)

data. Figure 2(b) is the Fourier spectra of the normalized acceleration histories. The normalized acceleration histories shown in Fig. 2(a) are input to N4SID. Figure 2(a) shows that the acceleration responses quickly reduce in case A3 due to the effect of a damper. Figure 2(b) shows that the peaks of the Fourier spectra of cases A1, A2, and A3 can be recognized up to around 100 Hz, 70 Hz, and 20

Hz, respectively. Due to the measurement error and damping, the peaks of the higher modes become unclear.

4.4.2 Dimension of system matrices

In the N4SID, the dimension of the system matrices is determined based on the singular values. The singular values were listed in descending order, and the order of the singular value just before the singular value became dramatically smaller was used as the order of the system matrices.

4.4.3 Natural frequency estimation results

Figure 2(c) shows the result of natural frequency estimation. The horizontal axis is the modal order, and the vertical axis is the ratio of estimated natural frequencies to true values. The accuracy is high if the vertical axis value is close to 1. In cases A1, A2, and A3, the natural frequencies up to the 35th mode (about 140 Hz), the 18th mode (about 70 Hz), and the 7th mode (35 Hz) are estimated, respectively. It is difficult to identify the natural frequencies of case A1 up to 140 Hz by visual inspection of Fig. 2(b). However, the N4SID detected the natural frequencies up to around 140 Hz with high accuracy. The overall accuracy is high. The estimation accuracy is quite high if there is no damper.

4.4.4 Damping factor estimation results

Figure 2(d) shows the result of damping factor estimation. The estimation accuracy is high except for the maximum order. The estimation error is less than 1% in case A1 without measurement error and less than 5% in A2 and A3 with measurement error, except for the maximum order.

4.4.5 Mode shape estimation results

We first estimated the mode shape at the four nodes with the N4SID, then normalized the mode shape with the largest one. The mode shape computed by the FEM is also normalized. Normalized mode shapes are compared for each mode. Figure 2(d) shows the result of mode shape estimation. The estimation accuracy is high for the lower modes in a case with no damper. In case A1, the estimation error is less than 0.01% for the modes lower than the 31st mode. In case A2 with measurement noise, the estimation error is within 3% for the modes lower than the 7th mode. However, the estimation accuracy is not high for the case with a damper. In case A3 with measurement noise and the damper, the estimation error is within 1% only for the 1st and the 3rd modes.

5. EXPERIMENTAL VERIFICATION

5.1 Overview

In this chapter, the validity of the N4SID is verified using the experimental results of an actual Nielsen-Lohse Bridge. A schematic diagram of the bridge is shown in Fig. 3(a). The bridge is a Nielsen-Lohse bridge, and a clamp connects the two intersecting cables. Vibration tests were conducted on two intersecting cables (case B), shown in red in Fig. 3(a). The cable lengths are shown in Fig. 3(b). The cables consist of 19 PC steel strands with a diameter of 12.7 mm bundled together and covered with a polyethylene sheath. Table 2 shows the material properties of the cables. The density per length and mass of a clamp shown in Table 2 is the design value. The tension and bending stiffness shown in Table 2 is estimated by the higher-order vibration method using the natural frequencies of each cable after removing the intersection clamp [9].

Figure 3(c) shows the position of excitation by the hammer and the position of the accelerometers. Cable 1 was hit in the out-of-plane direction, and the out-of-plane acceleration responses were measured with four accelerometers. The accelerometers were placed at 0.5 m intervals and numbered 1 to 4 from the bottom. Figures 4(a) and (b) show the measured acceleration histories and Fourier spectra. The measurement time interval is 0.00078125 s, and the duration is 25.6 s.

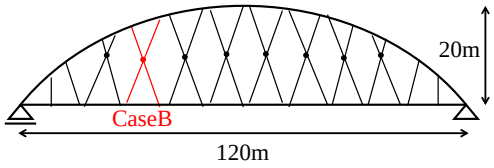

(a)Target Nielsen-Lohse Bridge and target cables

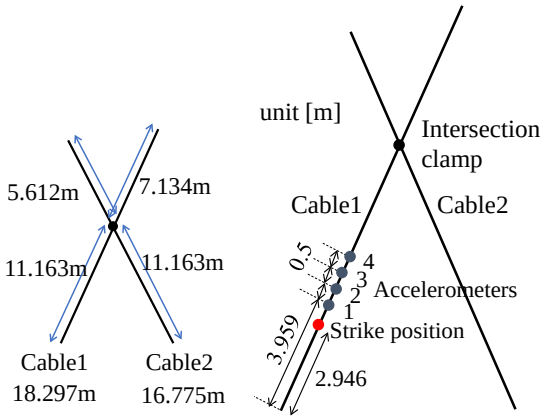

(b) Cable length (c) Measurement and striking position

Fig. 3 Experimental condition

Table 2 Material properties of two cables

Cable No.	Tension [kN]	Bending stiffness [kN·m^2]	Density per length [kg/m]	Mass of clamp [kg]
1	378.76	83.61	17.58	19.0
2	383.61	82.40		

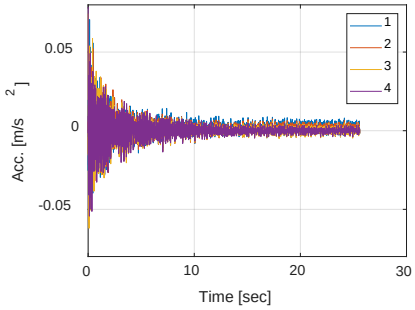

(a)Acceleration history

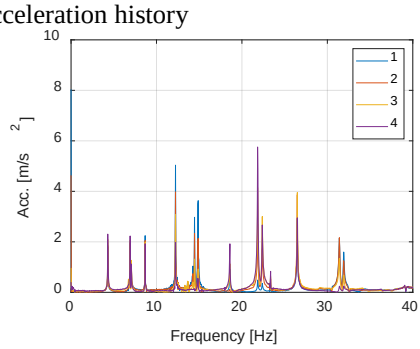

(b) Acceleration Fourier spectra

Fig. 4 Acceleration responses by experiment

5.2 Verification Method

Natural vibration characteristics are estimated using the N4SID. Furthermore, the natural frequencies and mode shapes are manually estimated from the acceleration Fourier spectra. The mode shapes were normalized to have a maximum value of 1. An eigenvalue analysis of the FEM is also performed using the material properties listed in Table 2. Since the damping factors of the two-intersecting cables were found to be very small, it was modeled with an undamped model. The cable was modeled with a tensioned Euler-Bernulli beam approximately 0.05 m in length. The computed natural frequencies and mode shapes by the FEM were considered true values. The mode shapes are normalized by dividing with the maximum value among the four measurement points.

5.3 Results

5.3.1 Natural frequency estimation results

Figure 5(a) compares the natural frequency estimation error between the N4SID and the manual estimation from the Fourier spectra. It was found that the N4SID has higher accuracy for most modes.

5.3.2 Mode shape estimation results

Figures 5(b), (c), and (d) are the comparison of the mode shapes among FEM, N4SID, and the manual estimation from the Fourier spectra for the 1st, 6th, and 7h modes. The mode shape plots by the N4SID are generally on the mode shape plot by the

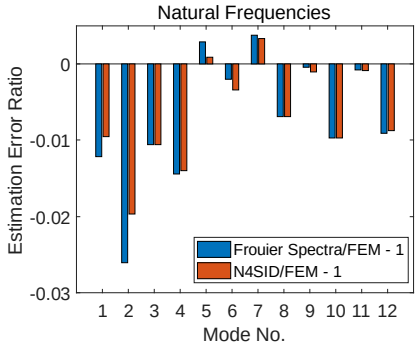

(a)Estimation error ratio of natural frequencies

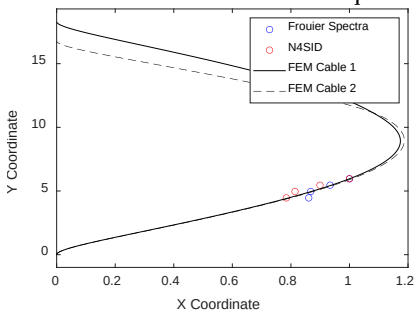

(b)Result of mode shape estimation (1st mode)

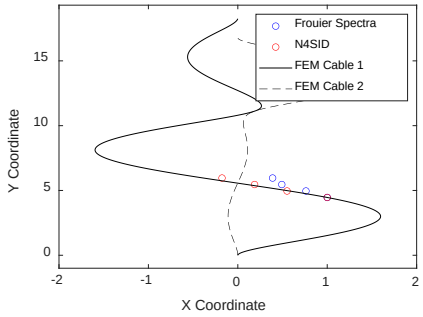

(c)Result of mode shape estimation (6th mode)

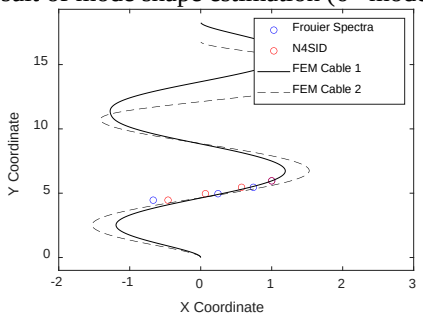

(d)Result of mode shape estimation (7th mode)

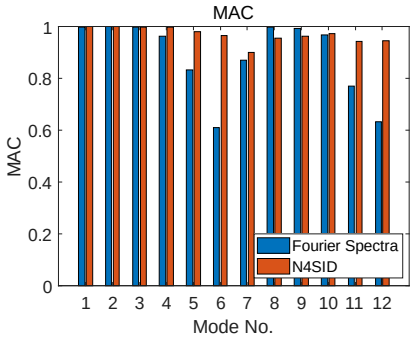

(e)MAC

Fig. 5 Estimation results from an experiment

FEM, whereas the mode shape plots obtained manually from the Fourier spectra are not always on the FEM mode shape plots. The above finding suggests that N4SID has higher accuracy.

Next, the Modal Assurance Criterion (MAC) was calculated to compare the accuracy quantitatively. MAC takes 1 when the two-mode shape vectors $\{\phi_A\}$ and $\{\phi_B\}$ are perfectly coincident, and 0 when they are orthogonal. The estimated mode shapes are substituted into $\{\phi_A\}$, and the mode shapes by the FEM are substituted into $\{\phi_B\}$.

$$\mathrm{MAC}(\phi_A, \phi_B) = \frac{|\{\phi_A\}^T\{\phi_B\}|^2}{(\{\phi_A\}^T\{\phi_A\})(\{\phi_B\}^T\{\phi_B\})} \quad (38)$$

Figure 5(e) compares the MAC between the N4SID and the manual estimation. The lowest MAC of manual estimation is 0.61 for the 6th mode, while the lowest MAC by the N4SID is 0.9 for the 7th mode. The N4SID tended to have a larger MAC and better agreement with the FEM analysis results.

6. CONCLUSIONS

This study investigated the applicability of the N4SID for the natural vibration characteristics estimation of bridge cables.

First, the applicability of the N4SID was investigated by the numerical simulation of a single cable with and without a damper. The following were observed.

1) The natural frequencies can be estimated with high accuracy, even with a measurement error of 5%. In the case of a cable with a damper, only estimation of lower modes is possible since the higher modes quickly dissipate. The measurement noise also reduces the number of natural frequencies to be identified.
2) The damping factors, except for the maximum order, could be accurately estimated. The estimation error is less than 1% in the case without measurement error and less than 5% in the case with measurement error.
3) The estimation accuracy of the mode shapes is high for the lower modes in the case with no damper. The estimation error is less than 0.01% for modes lower than the 31st mode in the case without measurement error and 3% for modes lower than the 7th mode in the case with measurement error. However, in the case with a damper, estimation error increased, and estimation error less than 1% was obtained only for the 1st and the 3rd modes.

Next, the applicability of the N4SID was investigated through the field measurement of the two-intersecting cables connected by a clamp on an actual Nielsen-Lohse bridge. It was found that natural frequencies and mode shapes estimated by the N4SID have higher accuracy than those by the manual estimation from the acceleration Fourier spectra. The superiority of the N4SID over the manual estimation from the Fourier spectra was shown.

7. ACKNOWLEDGMENTS

This work is supported by JSPS KAKENHI Grand Number 22K18830.

8. REFERENCES

[1] Gharehbaghi V.R., Farsangi E.N., Noori M., Yang T., Li S., Nguyen A., Málaga-Chuquitaype C., Gardoni P., Mirjalili S., A critical review on structural health monitoring: definitions, methods, and perspectives, Archives of computational methods in engineering, Vol. 29, 2022, pp.2209–2235.

[2] Furukawa A., Hagiwara K., Takahashi Y., Kiyono J., Quick earthquake damage evaluation of reinforced concrete pier using acceleration measurements, International Journal of GEOMATE, Vol. 21, Issue 86, 2021, pp.23-31. https://doi.org/10.21660/2021.86.j2210

[3] Furukawa A., Hirose K., Kobayashi R., Tension estimation method for cable with damper using natural frequencies, Frontiers in Built Environment, Vol.7, Article 603857, 2021, pp.1-17. https://doi.org/10.3389/fbuil.2021.603857

[4] Furukawa A., Suzuki S., Kobayashi R., Tension estimation method for cable with damper using natural frequencies with uncertain modal order, Frontiers in Built Environment, Vol.8, Article 812999, 2022, pp.1-17. https://doi.org/10.3389/fbuil.2022.812999

[5] Furukawa A., Suzuki S., Kobayashi R., Tension estimation method for cable with damper using natural frequencies and two-point mode shapes with uncertain modal order, Frontiers in Built Environment, Vol. 8, Article 906871, 2022, pp.1-19. https://doi.org/10.3389/fbuil.2022.906871

[6] Furukawa A., Hirose K., Kobayashi R., Tension estimation method for cable with damper and its application to real cable-stayed bridge. In: Wu, Z., Nagayama, T., Dang, J., Astroza, R. (eds) Experimental Vibration Analysis for Civil Engineering Structures. Lecture Notes in Civil Engineering, Vol.224, Springer, Cham, 2023, pp.379-390. https://doi.org/10.1007/978-3-030-93236-7_32

[7] Furukawa A., Yamada S., Kobayashi R., Tension estimation methods for two cables connected by an intersection clamp using natural frequencies, Journal of Civil Structural Health Monitoring, Vol.12, 2022, pp.339-360.

https://doi.org/10.1007/s13349-022-00548-6
[8] Furukawa A., Yamada S., Kobayashi R., Tension estimation methods for Nielsen-Lohse bridges using out-of-plane and in-plane natural frequencies, International Journal of GEOMATE, Vol.23, Issue 97, 2022, pp.1-11. https://doi.org/10.21660/2022.97.3235
[9] Furukawa A., Kozuru K., Suzuki M., Method for estimating tension of two Nielsen–Lohse bridge cables with intersection clamp connection and unknown boundary conditions, Frontiers in Built Environment, Vol. 8, Article 906871, 2022, pp.1-20. https://doi.org/10.3389/fbuil.2022.993958
[10] Chopra A.K., Dynamics of Structures: Theory and applications to earthquake engineering. Prentice-hall, Inc., Englewood Cliffs, N.J., 2007, pp.1-876.
[11] Cole H.A., On-line failure detection and damping measurement of aerospace structures by random decrement signatures. National Aeronautics and Space Administration, Vol. 2205, 1973, pp.1-75.
[12] Furukawa A., Otsuka H., Umebayashi F., Experimental study on changes in vibration characteristics due to structural damage, Proceedings of the JSCE Earthquake Engineering Symposium, Vol. 27, No. 19, 2005, pp.1-9. https://doi.org/10.11532/proee2005a.28.19
[13] Lee U., Shin J., A frequency response function-based structural damage identification method, Computers and Structures, Vol.80, 2002, pp.117-132.
[14] Verhaegen M., Subspace Techniques in System Identification. In: Baillieul, J., Samad, T. (eds) Encyclopedia of Systems and Control. Springer, London, 2014, pp.1-13. https://doi.org/10.1007/978-1-4471-5102-9_107-1.
[15] Yoshimoto R., Mita A., Online identification of structural parameters utilizing multi-input multi-output models, Journal of Structural and Construction Engineering (Transactions of AIJ), Vol. 68, Issue 574, 2003, pp.39-44.
[16] Nagano M., Hida T., Watanabe K., Tanuma T., Nakamura M., Ikawa N., Yasui M., Sakai S., Morishita T., Kawashima M., Dynamic characteristics of super high-rise residential buildings in Kanto and Kansai area based on strong motion records during the 2011 Off the Pacific Coast of Tohoku Earthquake, Journal of Japan Association for Earthquake Engineering, Vol.12, No.4, 2012, pp. 65-79.
[17] Hida T., Nagano M., Estimation accuracy of natural frequency and damping factor of building by system identification based on three subspace methods, Journal of Structural and Construction Engineering (Transaction of AIJ), Vol. 79, Issue 701, 2014, pp.923-932.
[18] Ishii Y., Yagi S., Yamada M., Sakaguchi G., Masuda H., Kataoka S., Damping characteristics of an entire highway bridge system estimated by system identification based on the subspace method, Journal of Japan Society of Civil Engineers, Vol. 78, Issue 4, 2022, pp. I_580-I_591.
[19] Overschee P.V., Moore B.D., N4SID: Subspace algorithms for the identification of combined deterministic-stochastic systems, Automatica, Vol. 30, Issue 1, 1994, pp.75-93.